Simple model for quantum chaos

Jaewan Kim and Wu-Pei Su
Department of Physics and Texas Center for Superconductivity, University of Houston, Houston, Texas 77204-5506
(Received 12 April 1993)

A simple second-quantized model exhibiting quantum chaos is introduced. Experimentally, this model could be realized as a triplet excitation of a molecule. Numerically, it requires only a minimal amount of computer time. Two cases of this model with and without inversion symmetry are discussed. The level spacing distribution of the case without inversion symmetry shows an especially close resemblance to the Wigner distribution. A related classical billiard model on a $1/r$-potential-energy surface is presented as a continuum extension of our model. The real-space representation of the Hamiltonian shows a self-similarity, whose fractal dimension is calculated to be 1.5.

PACS number(s): 05.45.+b, 03.65.−w, 71.20.Hk, 71.35.+z

The study of quantum chaos has followed as a natural sequel of the study of chaos in classical dynamics which has generated abundance of surprises, and has produced many impressive results [1–6]. While the study of classical chaos has benefited enormously from the use of simple maps and toy theoretical models and various simple experiments, the study of quantum chaos has relied heavily on extensive numerical calculations (e.g., [7]) and there are not many experiments for the study of quantum chaos. Steeb *et al.* [8] studied simple models related to the Hubbard model in condensed matter physics, and could not see the energy-level repulsion which seems to be the most promising criterion for quantum chaos.

In this paper, we construct a simple second-quantized model for quantum chaos which could be realized experimentally as a triplet excitation of a linear molecule, and demonstrate an aspect of quantum chaotic behavior of this system, i.e., energy-level repulsion, which requires only a minimal amount of computer time to get a high accuracy. We discuss a related classical billiard model as a continuum extension of our model. In addition, our model introduces a class of Hamiltonian matrix as a general feature of a many-body system, i.e., a self-similar Hamiltonian matrix.

Our model Hamiltonian describes the dynamics of two spinless electrons on a quasi-one-dimensional lattice, or more realistically, the dynamics of a triplet excitation of a linear molecule.

$$H = \sum_{i<j} [t_{ij}(c_i^\dagger c_j + c_j^\dagger c_i) + V_{ij} c_i^\dagger c_i c_j^\dagger c_j \,], \tag{1}$$

$$t_{ij} = t_0 \exp[-p(r_{ij} - a)], \tag{2}$$

$$V_{ij} = \frac{V_0}{r_{ij}}, \tag{3}$$

where $c_i^\dagger$ creates an electron on the ith site, c_j destroys an electron on the jth site. r_{ij} is the distance between the ith and the jth sites. t_{ij} describes the electron hopping integral between the ith and the jth sites, which decreases exponentially as the distance between them increases. V_{ij} describes the electron-electron interaction between the ith and the jth sites. For the sake of simplicity, we set the nearest neighbor hopping integral t_0 to be -1 and the lattice constant a to be 1. Then our model has two parameters, p and V_0.

This model is somewhat different from the Hubbard model which includes only the nearest neighbor hopping and the on-site Coulomb interaction. In our model, there is no on-site electron-electron interaction since the two electrons cannot occupy the same site. The extended hopping has been considered in tight-binding calculations of the C_{60} molecules [9,10]. The long range Coulomb interaction is important in the discussion of excitonic effect in conjugated polymers [11,12]. We show below that our model exhibits level repulsion and related level spacing statistics.

To calculate energy levels of this model Hamiltonian, we construct the Hilbert space of the two electrons on a 20-site chain. The total number of basis elements is ${}_{20}C_2 = 190$. A possible basis set consists of the following states:

$$|mn\rangle = c_m^\dagger c_n^\dagger |\,\rangle, \quad m < n \tag{4}$$

where $c_m^\dagger$ creates one electron on the mth site and $|\,\rangle$ denotes the vacuum. The restriction $m < n$ is given to avoid double counting. Our model Hamiltonian in this real-space representation provides very interesting contrasts with random matrices.

Since

$$\langle kl|c_i^\dagger c_j|mn\rangle = \langle\, |c_l c_k c_i^\dagger c_j c_m^\dagger c_n^\dagger|\,\rangle = \delta_{km}\delta_{li}\delta_{nj} + \delta_{ln}\delta_{ki}\delta_{mj} - \delta_{kn}\delta_{li}\delta_{mj} \quad i < j \tag{5}$$

and

$$\langle kl|c_i^\dagger c_i c_j^\dagger c_j|mn\rangle = \langle\, |c_l c_k c_i^\dagger c_i c_j^\dagger c_j c_m^\dagger c_n^\dagger|\,\rangle = \delta_{ki}\delta_{lj}\delta_{mi}\delta_{nj}, \quad i < j \tag{6}$$

1063-651X/94/50(2)/1019(5)/$06.00

$$\langle kl|H|mn\rangle = \begin{cases} \frac{V_0}{r_{kl}} & \text{if } k=m<l=n \\ -\exp[-p(r_{ln}-1)] & \text{if } k=m, l\neq n \\ -\exp[-p(r_{km}-1)] & \text{if } k\neq m, l=n \\ +\exp[-p(r_{lm}-1)] & \text{if } k=n, l\neq m \\ +\exp[-p(r_{kn}-1)] & \text{if } k\neq n, l=m \\ 0 & \text{otherwise.} \end{cases} \tag{7}$$

First, let us consider the case with inversion symmetry. All the lattice points are on a straight line. Figure 1 shows the energy levels of this Hamiltonian between 2.5 and 2.7 at $p = 0.8$ and V_0 varying from 0.5 to 1.1. We can see level repulsions as well as level crossings. Energy eigenfunctions have even or odd parities as expected from the inversion symmetry of our Hamiltonian. Opposite parity levels can cross each other, but same parity levels repel each other. This aspect is reflected in Fig. 2, which shows the energy-level spacing distribution for the energy levels from the 15th to the 190th at $V_0 = 0.8$ and $p = 0.8$. It shows a peak around 0 like a Poisson distribution, and another peak around 80% of the average level spacing like a Wigner distribution.

To gain additional insight we show in Fig. 3 a portion of the Hamiltonian matrix in real-space representation for $V_0 = 0.8$ and $p = 0.8$. Positive numbers are depicted as empty circles with area proportional to the numbers and negative numbers as solid circles. Hamiltonian matrices with random matrix elements are known to have a Wigner distribution for the level spacings. Our Hamiltonian matrix does not have entirely random elements. Among the 190^2 matrix elements, about 80% ($_{18}C_2/_{20}C_2$) are true zeros which are depicted by the gray squares in Fig. 3. There is a self-similarity among off-diagonal elements. This is a consequence of the hopping terms in (1), which are very common in many-body Hamiltonians. Diagonal elements are constructed from the interactions among the particles on various lattice sites. For example, we can calculate the fractal dimension of the region occupied by the nonzero elements. Let us call the 1×1 region at the right-bottom corner the first stage, $(1+2)\times(1+2)$ or 3×3 the second, $(1+2+3)\times(1+2+3)$ or 6×6 the third, and so on. Let $g(N)$ be the number of nonzero elements at the Nth stage. Then $g(1) = 1$, $g(2) = g(1) + 8 = 1 + 8 = 9$,

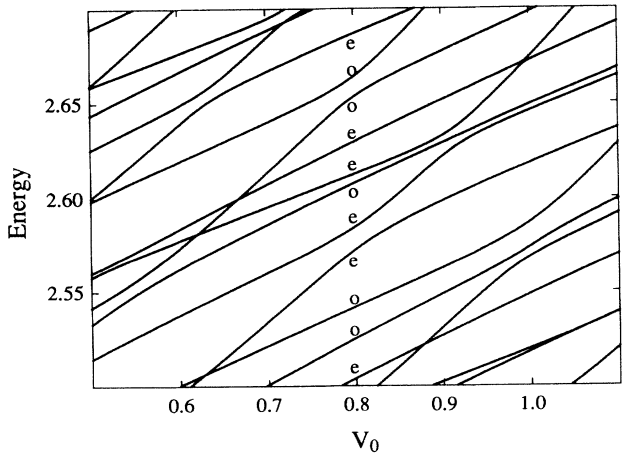

FIG. 1. The energy levels between 2.5 and 2.7 at $p = 0.8$ and V_0 varying from 0.5 to 1.1. Label e means even parity, and o odd parity. Same parity levels repel each other, but opposite parity levels can cross each other.

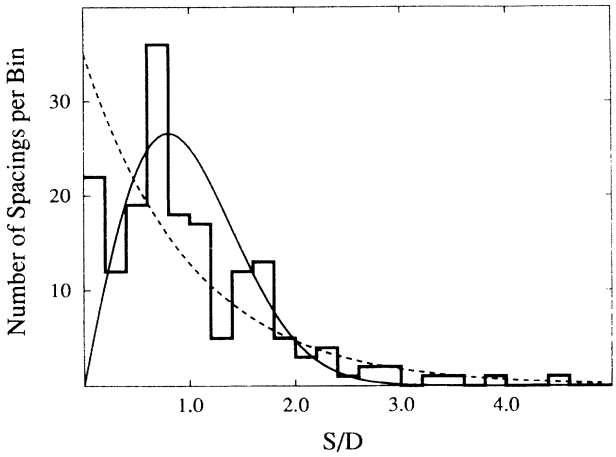

FIG. 2. The energy-level spacing distribution for energy levels from the 15th to the 190th at $V_0 = 0.8$ and $p = 0.8$. S is the level spacing and D is the average level spacing. Dashed line is the Poisson distribution and solid line is the Wigner distribution.

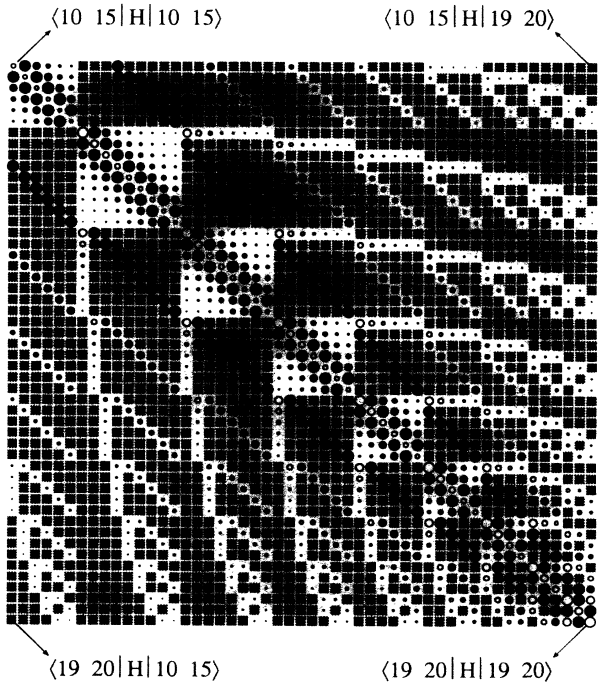

FIG. 3. A portion of the Hamiltonian matrix in real-space representation for $V_0 = 0.8$ and $p = 0.8$. Positive numbers are depicted by empty circles with area proportional to the numbers, and negative numbers by solid circles. True zeros are depicted by the gray squares. Left top corner element is $\langle 10\ 15|H|10\ 15\rangle$, left bottom $\langle 19\ 20|H|10\ 15\rangle$, right top $\langle 10\ 15|H|19\ 20\rangle$, and right bottom $\langle 19\ 20|H|19\ 20\rangle$.

$g(3) = g(2) + 21 = 30$, and so on. We can construct a recursion relation

$$g(N) = g(N-1) + N^2 + 4[(N-1) + (N-2) + \cdots + 1]$$
$$= g(N-1) + 3N^2 - 2N. \quad (8)$$

Thus

$$g(N) = N^3 + \frac{N^2}{2} - \frac{N}{2}. \quad (9)$$

At each stage, linear dimension of the matrix expands by N or as $\frac{1}{2}N(N+1)$, and the region of the nonzero elements grows as $N^3 + \frac{N^2}{2} - \frac{N}{2}$. Thus the fractal dimension of the region of the nonzero elements is

$$d = \lim_{N\to\infty} \frac{\ln\left(N^3 + \frac{N^2}{2} - \frac{N}{2}\right)}{\ln[\frac{1}{2}N(N+1)]} = 1.5\,. \quad (10)$$

It would be interesting to further study the consequence of this self-similarity in a renormalization scheme. But one thing to keep in mind is that Hamiltonians with hopping terms only or interaction terms only are integrable.

Now consider the second case without inversion symmetry. The lattice is straight from the first site up to the 13th site, then it is bent perpendicularly like a capital letter L to destroy the inversion symmetry. The structure of the Hamiltonian matrix is the same as the previous one except that some of the nonzero elements have somewhat different values because of changes in distances between lattice points.

Figure 4 shows the energy levels of this Hamiltonian between 2.7 and 3.1 at $p = 1$ and V_0 varying from 0.7 to 1.3. No level crossing is observed here, as expected from the lack of symmetry. If there were no extended hopping or long range interactions, this kind of geometry change would not make any difference.

Figure 5 shows an eigenfunction with energy $E \approx 2.72$ at $V_0 = 1$ and $p = 1$. Even though this model is purely quantum mechanical, this eigenfunction strongly reminds us of Heller's *scars* of classically periodic orbits on quantum eigenfunctions in chaotic systems [13–15]. We can think of a periodic orbit related to this eigenfunction: initially two electrons trapped between the 13th and 20th sites are residing on the 14th and 16th sites repelling each other; then they separate and bounce off the 13th and 20th sites and head toward each other again, settling down on the 17th and 19th sites for some time and separate and so on.

Figure 6 shows the level spacing distribution for the energy levels from the 18th to the 190th at $V_0 = 1$ and $p = 1$. Even though about 80% of the matrix elements are true zeros as in the case with inversion symmetry, it shows close resemblance to Wigner distribution like the random matrices.

Since our model describes two electrons in a quasi-one-dimensional system, it must be related to a one-particle two-dimensional system. Since we have two fermions and the wave function should have odd parity for the exchange of the coordinates of the two electrons, we need only the upper triangular part of the square as in Fig. 5

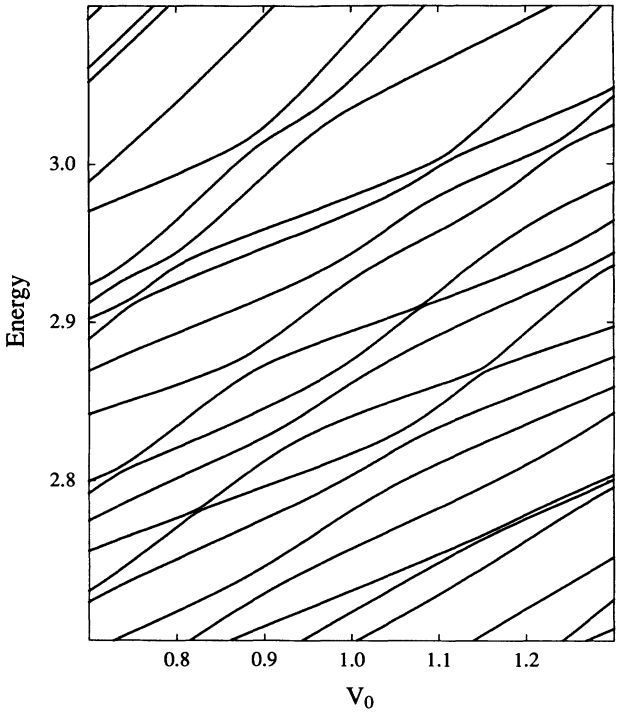

FIG. 4. The energy levels between 2.7 and 3.1 at $p = 1$ and V_0 varying from 0.7 to 1.3 without inversion symmetry. No level crossing is observed. Apparent crossings are due to the resolution.

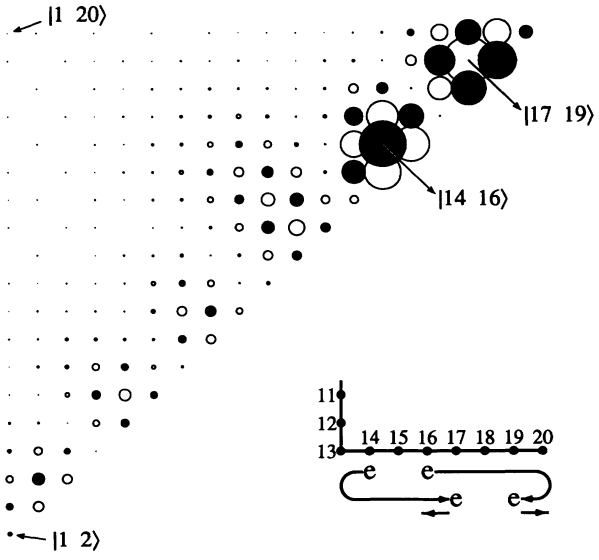

FIG. 5. The real-space representation of an eigenfunction with energy $E \approx 2.72$ at $V_0 = 1$ and $p = 1$ and the related periodic motion of two electrons. The probability amplitude of $|m\ n\rangle$ is depicted by an empty circle with a radius proportional to the amplitude if it is positive, and by a solid circle if negative. So the area is proportional to the probability.

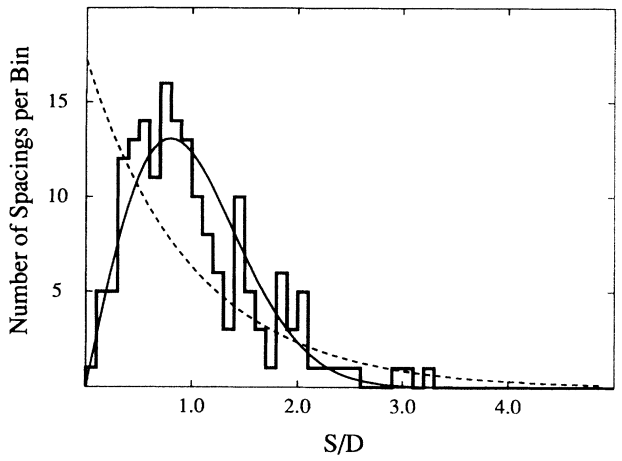

FIG. 6. The energy-level spacing distribution for the energy levels from the 18th to the 190th at $V_0 = 1$ and $p = 1$ without inversion symmetry. S is the level spacing and D is the average level spacing. Dashed line is the Poisson distribution and solid line is the Wigner distribution.

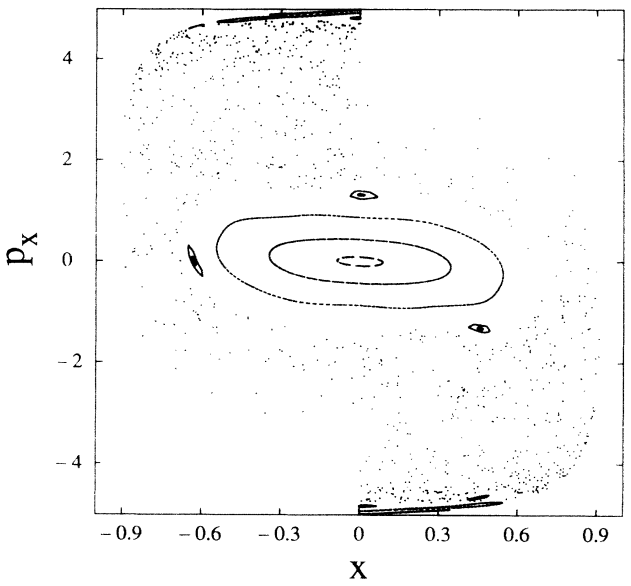

FIG. 7. Poincaré surface of section for a billiard ball with $E = 14.5$ in an isosceles right triangle with a $1/r$-potential energy, where r is the distance from the hypotenuse. The abscissa is for the x coordinate of the billiard ball at the moment of collision with the sides. The ordinate is for the momentum of the billiard ball in the x direction just after the collision.

instead of a whole square. The first neighbor hopping terms are in exactly the same form as the discretization of a kinetic energy term, and the diagonal terms due to the interaction between electrons translate into a potential-energy term on a two-dimensional plane with the distance from the hypotenuse being the distance between the two electrons.

In other words, our model can be extended to a continuum limit by neglecting the hopping terms except the first neighbor hoppings and by expanding the size of the lattice to infinity: a billiard ball in an isosceles right triangle with a potential energy rising toward the hypotenuse as $1/r$, where r is the distance from the hypotenuse. Take the vertex of the right angle in the isosceles right triangle as the origin, the line starting from the origin bisecting the hypotenuse as y axis, and the line perpendicular to this y axis and passing through the origin as x axis. If the distance between the origin and the hypotenuse is set to 1, then the distance between the electrons or the distance from the hypotenuse becomes $1 - y$. Thus the Hamiltonian of the continuum model becomes

$$H = \frac{1}{2}\left(p_x^2 + p_y^2\right) + \frac{1}{1-y}, \tag{11}$$

with a boundary

$$y = x,\ y = -x,\ y = 1.$$

Without a potential-energy variation, this billiard ball system is integrable [16]. With a linear potential energy, i.e., the billiard table tilted toward the corner of the right angle, it is still integrable. But with a $1/r$-potential energy as in our model, its classical dynamics shows chaotic behavior as the surface of section in Fig. 7 indicates. In Fig. 7, we plotted the surface of section for six initial conditions with the same energy. While five of the initial conditions give continuous invariant curves, evolution of one initial condition fills a wide area of the phase space quite randomly.

In conclusion, we have introduced a second-quantized model of two spinless electrons on a quasi-one-dimensional lattice, which could describe triplet excitations in a linear molecule. When the system possesses inversion symmetry, energy levels with opposite parity can cross each other, while energy levels with same parity repel each other. Thus the energy-level spacing distribution shows a mixture of Poisson and Wigner distributions. With the inversion symmetry removed from this model, no energy-level crossings were observed and the energy-level spacing distribution shows close resemblance to the Wigner distribution despite the fact that the matrix elements are far from random.

Experimentally, our model is feasible in one-dimensional systems such as conducting polymers or quantum wires. Numerically, this model is simple and comparable to the simple maps and toy models in the study of classical chaos. Thus our model Hamiltonian represents a very simple model for quantum chaos and introduces a self-similar Hamiltonian matrix as a new class of matrices. As such it deserves further explorations.

This study was partially supported by the Robert A. Welch Foundation and the Texas Center for Superconductivity. J.K. appreciates Dr. R. H. G. Helleman and Dr. Swan Kim for their recommendations to the Les Houches Session LII Chaos and Quantum Physics, and lecturers and colleagues in that session, Dr. P. Cvitanović, Dr. C. S. Ting, Dr. G. Gunaratne, and Dr. G. Levine for many useful discussions. W.P.S. acknowleges the donors of the Petroleum Research Fund administered by the American Chemical Society for partial support of the research.

[1] B. Eckhardt, Phys. Rep. **163**, 205 (1988).
[2] *Chaos and Quantum Physics*, edited by M.-J. Giannoni, A. Voros, and J. Zinn-Justin (North-Holland, Amsterdam, 1991).
[3] M. C. Gutzwiller, *Chaos in Classical and Quantum Mechanics* (Springer, New York, 1990).
[4] F. Haake, *Quantum Signatures of Chaos* (Springer, Berlin, 1991).
[5] L. E. Reichl, *The Transition to Chaos* (Springer, New York, 1992).
[6] R. V. Jensen, Nature (London) **355**, 311 (1992).
[7] G. Montambaux, D. Poilblanc, J. Bellissard, and C. Sire, Phys. Rev. Lett. **70**, 497 (1993).
[8] W.-H. Steeb, C. M. Villet, and A. Kunik, Phys. Rev. A **32**, 1232 (1985).
[9] Dandan Guo and S. Mazumdar, Synth. Metals **49-50**, 175 (1992).
[10] J. Kim (unpublished).
[11] S. Abe, M. Schreiber, and W.-P. Su, Chem. Phys. Lett. **192**, 425 (1992).
[12] S. Abe, M. Schreiber, W.-P. Su, and J. Yu, Phys. Rev. B **45**, 9432 (1992).
[13] E. J. Heller, Phys. Rev. Lett. **53**, 1515 (1984).
[14] E. J. Heller, in *Chaos and Quantum Physics* (Ref. [2]), pp. 547–664.
[15] S. Tomsovic and E. J. Heller, Phys. Rev. Lett. **70**, 1405 (1993).
[16] M. V. Berry and M. Wilkenson, Proc. R. Soc. London, Ser. A **392**, 15 (1984).

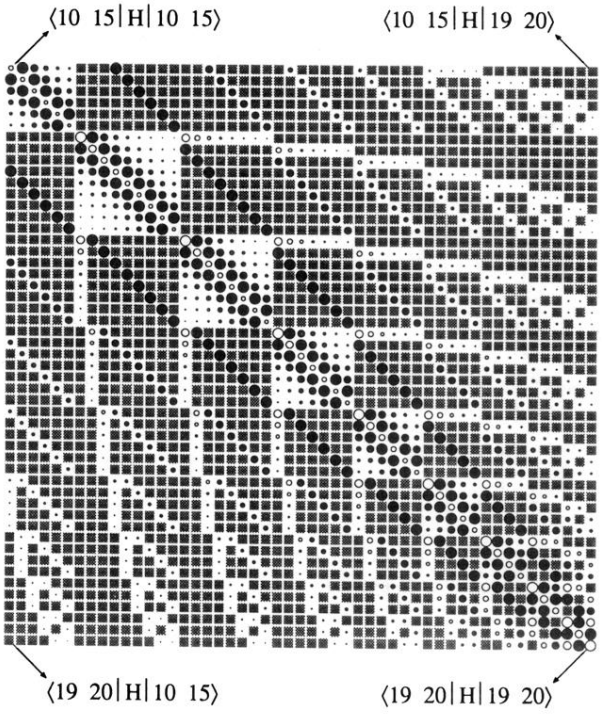

FIG. 3. A portion of the Hamiltonian matrix in real-space representation for $V_0 = 0.8$ and $p = 0.8$. Positive numbers are depicted by empty circles with area proportional to the numbers, and negative numbers by solid circles. True zeros are depicted by the gray squares. Left top corner element is $\langle 10\ 15|H|10\ 15\rangle$, left bottom $\langle 19\ 20|H|10\ 15\rangle$, right top $\langle 10\ 15|H|19\ 20\rangle$, and right bottom $\langle 19\ 20|H|19\ 20\rangle$.